The Astrophysical Journal, 826:141 (6pp), 2016 August 1 doi:10.3847/0004-637X/826/2/141

THE BLACK HOLE CENTRAL ENGINE FOR ULTRA-LONG GAMMA-RAY BURST 111209A AND ITS ASSOCIATED SUPERNOVA 2011KL

He Gao[1], Wei-Hua Lei[2], Zhi-Qiang You[1], and Wei Xie[2]
[1] Department of Astronomy, Beijing Normal University, Beijing 100875, China; gaohe@bnu.edu.cn
[2] School of Physics, Huazhong University of Science and Technology, Wuhan, 430074, China; leiwh@hust.edu.cn
Received 2016 January 15; revised 2016 April 25; accepted 2016 May 13; published 2016 July 27

ABSTRACT

Recently, the first association between an ultra-long gamma-ray burst (GRB) and a supernova was reported, i.e., GRB 111209A/SN 2011kl, enabling us to investigate the physics of central engines or even progenitors for ultra-long GRBs. In this paper, we inspect the broadband data of GRB 111209A/SN 2011kl. The late-time X-ray light curve exhibits a GRB 121027A-like fallback bump, suggesting a black hole (BH) central engine. We thus propose a collapsar model with fallback accretion for GRB 111209A/SN 2011kl. The required model parameters, such as the total mass and radius of the progenitor star, suggest that the progenitor of GRB 111209A is more likely a Wolf–Rayet star instead of a blue supergiant, and the central engine of this ultra-long burst is a BH. The implications of our results are discussed.

Key words: accretion, accretion disks – black hole physics – gamma-ray burst: individual (GRB 111209A)

1. INTRODUCTION

Recently, "ultra-long bursts," a subclass of gamma-ray bursts (GRBs) with unusually long central engine activity (∼hours) compared to typical GRBs (tens of seconds), have been paid great attention (Gendre & Stratta 2013; Stratta et al. 2013; Virgili et al. 2013; Levan et al. 2014; Greiner et al. 2015). In some references, the "ultra-long" GRBs referred to the GRBs with γ-ray duration T_{90} extending to $\sim 10^3$ s or even larger[3] (Gendre & Stratta 2013; Stratta et al. 2013; Virgili et al. 2013; Levan et al. 2014). Some authors (Zhang et al. 2014; Gao & Mészáros 2015), on the other hand, argue that T_{90} is not a reliable measure for defining "ultra-long" GRBs, taking into account the prolonged central engine activity time of some GRBs, indicated by flares (Burrows et al. 2005; Zhang et al. 2006; Margutti et al. 2011) and shallow decay plateaus (Liang et al. 2007; Troja et al. 2007) in the early X-ray afterglow light curves. They propose to redefine the burst duration as $t_{\rm burst}$ by taking into account both γ-ray and the aforementioned X-ray light-curve features. Based on both observational analysis and numerical simulations, they found that bursts with duration T_{90} of order 10^3 s can be reproduced with a normal central engine, while bursts with $t_{\rm burst} > 10^4$ s require an extended central engine activity and may be classified in the "ultra-long" population (Zhang et al. 2014; Gao & Mészáros 2015).

Even with the lack of a clear definition, it is generally considered that the ultra-long GRBs may have either a special central engine or a special progenitor (Levan et al. 2014). For instance, some authors (Gendre & Stratta 2013; Nakauchi et al. 2013; Levan et al. 2014) proposed a blue supergiant-like progenitor for ultra-long GRBs (Mészáros & Rees 2001; Nakauchi et al. 2013), considering that their much larger radii could naturally explain the unusually long durations. On the other hand, it has also been proposed that the ultra-long GRBs may have a special central engine, such as a strongly magnetized millisecond neutron star (a magnetar; Levan et al. 2014; Greiner et al. 2015). Research on the physical origin of ultra-long GRBs would potentially promote our understanding of the central engine and progenitor of GRBs.

[3] Although no clear boundary line has been defined yet.

Most recently, Greiner et al. (2015) reported the first discovered association between an ultra-long GRB and a supernova (SN), i.e., GRB 111209A/SN 2011kl. Based on the observed properties of SN 2011kl, such as its spectra and light-curve shape, they rule out a blue supergiant progenitor and a tidal disruption interpretation for GRB 111209A. Nevertheless, based on the unexpected high luminosity of SN 2011kl, which is intermediate between canonical overluminous GRB-associated SNe and superluminous SNe (Quimby et al. 2011; Gal-Yam 2012), they suggest that ^{56}Ni is not responsible for powering the luminosity of SN 2011kl, but an additional energy input is required. They thus propose that the central engine of GRB 111209A might be a millisecond magnetar.

Considering the comprehensive observations of GRB 111209A/SN 2011kl, especially that the late-time X-ray light curve of GRB 111209A exhibits a GRB 121027A-like fallback bump (Wu et al. 2013), rather than obeying the dipole radiation profile, the central engine of GRB 111209A is more like a black hole (BH) instead of a magnetar. The question is, could the BH central engine serve as the energy reservoir to power the abnormally luminous SN 2011kl? In this work, we intend to interpret the broadband data of GRB 111209A/SN 2011kl within the collapsar model: the GRB central engine is a BH; a fraction of the materials in the envelope would fall back and reactivate the accretion onto the BH, tapping the spin energy of the BH to give rise to the unusually long central engine activity timescale; the energy and angular momentum could also be extracted magnetically from the revived accretion disk, depositing energy into the SN ejecta to give rise to the unusually high luminosity of SN 2011kl. In Section 2, we describe the observational features of GRB 111209A. A general picture of the fallback accretion model is given in Section 3, and we apply this model to the broadband data of GRB 111209A/SN 2011kl in Section 4. In Section 5, we briefly summarize our results and discuss the implications.

2. OBSERVATIONAL FEATURES OF GRB 111209A

GRB 111209A was discovered at $T_0 = 2011{:}12{:}09{-}07{:}12{:}08$ UT on 2011 December 9 by the Burst Alert Telescope (BAT) on board *Swift* and was later accurately located by XRT at a position

of R.A.(J2000) = $00^h57^m22^s.63$ and decl.(J2000) = $-46^d48'03''.8$, with an estimated uncertainty of $0''.5$ (Hoversten et al. 2011). GRB 111209A showed an extraordinarily long prompt duration and was monitored up to $T_0 + 1400$ s until BAT entering the orbital gap region. It was also detected by the Konus detector on the *Wind* spacecraft (Golenetskii et al. 2011). As shown in the ground data analysis of the Konus-*Wind* instrument, GRB 111209A was recorded with a continuous coverage extending from 5400 s before to 10,000 s after the *Swift* trigger T_0.

Both Very Large Telescope/X-shooter (2011 December 10 at 1:00 UT) and Gemini-N/GMOS-N detected the early spectroscopy of the transient optical light of GRB 111209A. A redshift of $z = 0.677$ was suggested by the identification of absorption lines and emission lines from the host galaxy (Vreeswijk et al. 2011). Based on the Konus-*Wind* results, GRB 111209A had a fluence of $(4.86 \pm 0.61) \times 10^{-4}$ erg cm^{-2} (Golenetskii et al. 2011), inferring an isotropic gamma-ray energy release $E_{\gamma,\rm iso} = 4\pi D_L^2 f_\gamma/(1+z) = 5.54 \pm 0.70 \times 10^{53}$ erg. Here we adopt the concordance cosmology with $\Omega_m = 0.27$, $\Omega_\Lambda = 0.73$, and $h_0 = 0.71$.

Swift/XRT observations started at 425 s after the BAT trigger (Hoversten et al. 2011), revealing a bright afterglow mainly with several components:

1. An initial plateau phase overlapping with the prompt γ-ray emission.
2. After an observational gap, from 3×10^3 s to $\sim 10^4$ s, the light curve rapidly rises back and then gradually steepens to a "steep decay" phase with decay index of $\sim$5, behaving very much like the GRB 121027A-like fallback bump (Wu et al. 2013).
3. At very late time ($\sim 10^5$ s), the tail of steep decay phase is superposed by another power-law component with decay index of $\sim$1.5, which is usually denoted as "normal decay" phase in the canonical picture of X-ray afterglow (Zhang et al. 2006).

The afterglow of GRB 111209A was also clearly detected in the optical–UV band by *Swift*/UVOT and other ground-based instruments, such as the TAROT-La Silla (Klotz et al. 2011) and the seven-channel optcial/near-infrared imager GROND (Kann et al. 2011). After the prompt optical flashes, the earlier optical afterglow shows a normal power-law decay until day 15. And then, the optical light curve starts to deviate from the power-law decay and remains essentially flat between days 15 and 30. After day 30, the light curve starts to decay again, approaching the host-galaxy level. Most recently, based on its temporal and spectral features, this excess emission is identified as an SN, designated SN 2011kl, associated with GRB 111209A (Greiner et al. 2015). The bolometric peak luminosity of SN 2011kl is intermediate between canonical overluminous GRB-associated SNe and superluminous SNe.

3. FALLBACK ACCRETION MODEL

In this work, we intend to use the collapsar model to interpret the broadband afterglow data of GRB 111209A. The physical picture is as follows: the progenitor star has a core-envelope structure, as is common in stellar models. The bulk of the mass in the core part collapses into a rapidly spinning BH, and the rest mass forms a surrounding accretion disk. The GRB prompt emission can be powered by the Blandford & Znajek (1977, hereafter BZ) mechanism, in which the spin energy of the BH is extracted via the open field lines penetrating the event horizon. An alternative mechanism for powering the GRB jet is the neutrino annihilation process, which is too "dirty" and inffective to account for long-term activity of GRBs, like ultra-long GRBs (Fan et al. 2005; Lei et al. 2009, 2013; Liu et al. 2015). The energy and angular momentum could also be extracted magnetically from accretions disks, by field lines that leave the disk surface and extend to large distance, centrifugally launching a baryon-rich wide wind/outflow through the Blandford–Payne (Blandford & Payne 1982, hereafter BP) mechanism. The bounding shock responsible for the associated SN and the BP outflow would transfer kinetic energy to the envelope materials. During the fallback, only a portion of the fallback mass accretes onto the BH, while the rest is ejected in a disk wind (Kumar et al. 2008a, 2008b). The more energetic the SN shock, the less envelope material falls back into the center. For a parcel of gas of the progenitor star at radius $r_{\rm fb}$, the fallback time could be estimated as $t_{\rm fb} \sim (\pi^2 r_{\rm fb}^3/8GM_\bullet)^{1/2}$, where $M_\bullet$ is the BH mass. The fallback of the envelope materials may form a new accretion disk, powering the shallow decay phase or late flares seen in X-ray afterglow. The BP outflow from the new disk would further deposit energy into the SN ejecta.

Based on some analytical and numerical calculations, the fallback accretion rate initially increases with time as $\dot{M}_{\rm early} \propto t^{1/2}$ until it reaches a peak value at $t_{\rm p}$ (MacFadyen et al. 2001; Zhang et al. 2008; Dai & Liu 2012). And then the late-time fallback accretion behavior would follow $\dot{M}_{\rm late} \propto t^{-5/3}$, as suggested by Chevalier (1989) until time t_b, when most of the fallback materials were accreted and the accretion behavior could be described with $\dot{M}_{\rm final} \propto t^{-\alpha}$, where α depends on the stellar structure and rotation rate of progenitor star.[4] We use a three-segment broken power-law function of time to describe the evolution of the fallback accretion rate as

$$\dot{M} = \dot{M}_{\rm p}\left[\frac{1}{2}\left(\frac{t-t_0}{t_{\rm p}-t_0}\right)^{-1/2} + \frac{1}{2}\left(\frac{t-t_0}{t_{\rm p}-t_0}\right)^{5/3}\right]^{-1} \times \left[1 + \left(\frac{t-t_0}{t_{\rm b}-t_0}\right)^{\alpha-5/3}\right]^{-1}, \quad (1)$$

where t_0 is the starting time of fallback accretion (henceforth, time is defined in the cosmologically local frame).

Consider a Kerr BH with mass $M_\bullet$ (or dimensionless mass $m_\bullet = M_\bullet/M_\odot$) and angular momentum $J_\bullet$. The BZ jet power is (Lee et al. 2000; Li 2000; Wang et al. 2002; McKinney 2005; Lei et al. 2008; Lei & Zhang 2011; Lei et al. 2013)

$$L_{\rm BZ} = 1.7 \times 10^{50} a_\bullet^2 m_\bullet^2 B_{\bullet,15}^2 F(a_\bullet) \ {\rm erg\ s^{-1}}, \quad (2)$$

where $a_\bullet = J_\bullet c/(GM_\bullet^2)$ is the BH spin parameter and $F(a_\bullet) = [(1+q^2)/q^2][(q+1/q)\arctan q - 1]$, with $q = a_\bullet/(1+\sqrt{1-a_\bullet^2})$. $B_\bullet$ is the magnetic field strength threading the BH horizon. Since the magnetic field on the BH is supported by the surrounding disk, one can estimate its value by equating the magnetic pressure on the horizon to the ram pressure of the

[4] In this work, the value of α is inferred from the X-ray afterglow steep decay index.

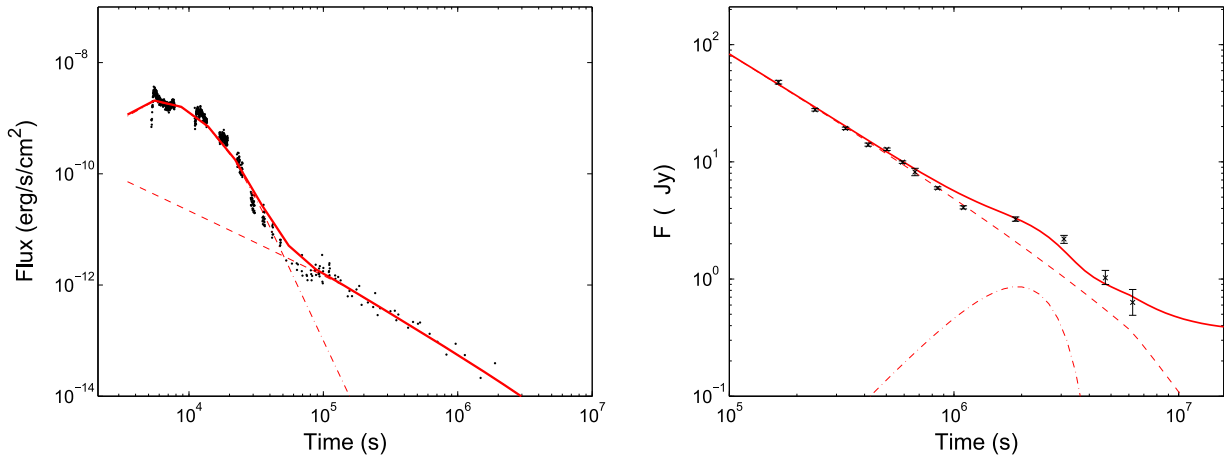

Figure 1. Modeling results for the XRT range (left panel) and *r*-band (right panel) light curve of GRB 111209A. The observed data are exhibited with points, and the theoretical modeling is shown with solid lines. The thin dashed line denotes the external shock component, and the dot–dashed line in the left (right) panel denotes the BZ-powered radiation according to the fallback disk (the BP-outflow-powered SN component). For optical data, a constant host-galaxy emission is invoked (Greiner et al. 2015).

accretion flow at its inner edge (e.g., Moderski et al. 1997),

$$\frac{B_{\bullet}^2}{8\pi} = P_{\rm ram} \sim \rho c^2 \sim \frac{\dot{M}c}{4\pi r_{\bullet}^2}, \quad (3)$$

where $r_{\bullet} = (1+\sqrt{1-a_{\bullet}^2})r_{\rm g}$ is the radius of the BH horizon, and $r_{\rm g} = GM_{\bullet}/c^2$. We can then rewrite the BZ power as a function of mass accretion rate as

$$L_{\rm BZ} = 9.3\times10^{53} a_{\bullet}^2 \dot{m} X(a_{\bullet})\ {\rm erg\ s^{-1}}, \quad (4)$$

and

$$X(a_{\bullet}) = F(a_{\bullet})/(1+\sqrt{1-a_{\bullet}^2})^2. \quad (5)$$

The observed X-ray luminosity is connected to the BZ power via the X-ray radiation efficiency η and the jet beaming factor $f_{\rm b}$, i.e.,

$$\eta L_{\rm BZ} = f_{\rm b} L_{\rm X,iso}. \quad (6)$$

The BP outflow luminosity could be estimated as (Armitage & Natarajan 1999)

$$L_{\rm BP} = \frac{(B_{\rm ms}^{\rm P})^2 r_{\rm ms}^4 \Omega_{\rm ms}^2}{32c} \quad (7)$$

where $B_{\rm ms}^{\rm P}$ and $\Omega_{\rm ms}$ are the poloidal disk field and the Keplerian angular velocity at inner stable circular orbit radius ($r_{\rm ms}$). Here we define $R_{\rm ms} = r_{\rm ms}/r_{\rm g}$ as the radius of the marginally stable orbit in terms of $r_{\rm g}$. The expression for $R_{\rm ms}$ is (Bardeen et al. 1972)

$$R_{\rm ms} = 3 + Z_2 - [(3-Z_1)(3+Z_1+2Z_2)]^{1/2}, \quad (8)$$

for $0 \leqslant a_{\bullet} \leqslant 1$, where $Z_1 \equiv 1 + (1-a_{\bullet}^2)^{1/3}[(1+a_{\bullet})^{1/3} + (1-a_{\bullet})^{1/3}]$, $Z_2 \equiv (3a_{\bullet}^2 + Z_1^2)^{1/2}$. The quantity $\Omega_{\rm ms}$ is given by

$$\Omega_{\rm ms} = \frac{1}{M_{\bullet}/c^3(\chi_{\rm ms}^3 + a_{\bullet})} \quad (9)$$

where $\chi_{\rm ms} \equiv \sqrt{r_{\rm ms}/M_{\bullet}}$. Following Blandford & Payne (1982), $B_{\rm ms}^{\rm P}$ could be estimated as

$$B_{\rm ms}^{\rm P} = B_{\bullet}(r_{\rm ms}/r_H)^{-5/4} \quad (10)$$

where $r_H = M_{\bullet}(1+\sqrt{1-a_{\bullet}^2})$ is the horizon radius of the BH.

The photospheric luminosity of SNe powered by a variety of energy sources (e.g., radioactive ^{56}Ni decay, BP power injection, etc.) could be expressed as (Arnett 1982; Wang et al. 2015a, 2015b)

$$L(t) = \frac{2}{\tau_m} e^{-\left(\frac{t^2}{\tau_m^2}+\frac{2R_0 t}{v\tau_m^2}\right)}(1-e^{-\tau_\gamma(t)})\int_0^t e^{\left(\frac{t't'^2}{\tau_m^2}+\frac{2R_0 t'}{v\tau_m^2}\right)} \times\left(\frac{R_0}{v\tau_m}+\frac{t'}{\tau_m}\right)L_{\rm inj}(t')dt'\ {\rm erg\ s^{-1}}, \quad (11)$$

where R_0 is the initial radius of the progenitor, which could be taken as zero to largely simplify the above equation since it is very small compared to the radius of the ejecta. τ_m is the effective light-curve timescale, which reads

$$\tau_m = \left(\frac{2\kappa M_{\rm ej}}{\beta v c}\right)^{1/2}, \quad (12)$$

where κ, $M_{\rm ej}$, and v are the Thomson electron scattering opacity, the ejecta mass, and the expansion velocity of the ejecta. $\beta \simeq 13.8$ is a constant that accounts for the density distribution of the ejecta (Wang et al. 2015a, 2015b). $L_{\rm inj}$ is the generalized energy source. $(1-e^{-\tau_\gamma(t)})$ reflects the γ-ray trapping rate, with $\tau_\gamma(t) = At^{-2}$ being the optical depth to γ-rays (Chatzopoulos et al. 2009, 2012). Provided that the SN ejecta has a uniform density distribution ($M_{\rm ej} = (4/3)\pi\rho R^3$, $E_{\rm K} = (3/10)M_{\rm ej}v^2$), the characteristic parameter A could be estimated as

$$A = \frac{3\kappa_\gamma M_{\rm ej}}{4\pi v^2} = 4.75\times10^{13}\left(\frac{\kappa_\gamma}{0.1\ {\rm cm^2\ g^{-1}}}\right) \times\left(\frac{M_{\rm ej}}{M_\odot}\right)\left(\frac{v}{10^9\ {\rm cm\ s^{-1}}}\right)^{-2}{\rm s^2}, \quad (13)$$

where κ_γ is the opacity to γ-rays.

As argued in Greiner et al. (2015), radioactive ^{56}Ni decay could not be responsible for the luminosity of SN 2011kl. Here

we take that

$$L_{\rm inj} \simeq L_{\rm BP}. \quad (14)$$

4. APPLICATION TO GRB 111209A

In the following, we apply the above fallback accretion model to fit the broadband data of GRB 111209A, as presented in Figure 1. Table 1 summarize the values of the parameters adopted in the model. We find that the broadband data of GRB 111209A could be well explained with all standard parameter values.

The early X-ray light curve (from 3000 s to 5×10^4 s) could be well interpreted with the BZ power induced by the fallback disk. We focus on the overall shape of the X-ray light curve. The flare-like variations during this phase could be due to the fragmentation during the fallback phase (King et al. 2005). The contribution from the GRB afterglow emission is initially outshone by the BZ power and emerges later ($>5 \times 10^4$ s) to account for the late-time normal decay light curve. As shown in Figure 1, the early optical data may come from the GRB afterglow emission, while the late optical data, i.e., the SN 2011kl component, could be dominated by the emission from a BP-process-powered SN.

In the interpretation for the afterglow component, the jet isotropic kinetic energy E_k of 7.6×10^{52} erg and the ambient medium density n of 1 cm^{-3} are adopted.[5] The fitting results depend weakly on the values of initial Lorentz factor (Γ_0) and half opening angle (θ) of the jet. The microphysics shock parameters (e.g., ϵ_e, ϵ_B, and p) are all chosen as their commonly used values in GRB afterglow modeling (see Gao et al. 2013; Kumar & Zhang 2015, for a review). To compare with the observations of the X-ray bump in GRB 111209A, we carried out numerical calculation for the time evolution of the BZ power. The radiation efficiency $\eta = 0.05$ is taken in our calculation. The BH is initially set up with a mass $m_\bullet = 3$ and a spin $a_\bullet = 0.9$. The fallback accretion starts at $t_0 = 3000/(1+z)$ s, peaks at $t_{\rm p} = 8000/(1+z)$ s, and breaks around $t_{\rm b} = 1.8 \times 10^4/(1+z)$ s. The outermost radius of the fallback material could be essentially estimated as $r_{\rm fb} \sim (8GM_\bullet t_{\rm b}^2/\pi^2)^{1/3} = 3.2 \times 10^{11}$ cm, which is smaller than the typical radius of a blue supergiant star (Nakauchi et al. 2013). To achieve the fitness of the data, the late-time accretion rate decay index $\alpha = 5$ is required. For the SN ejecta, we take the standard values for its mass ($M_{\rm ej} \sim 3M_\odot$), initial velocity ($v_i = 0.06c$), and the effective opacity $\kappa = 0.06$ cm^2 g^{-1} (Lyman et al. 2016). Note that these ejecta parameters suffer severe degeneracy, which could be justified by Equation (12).

From Equations (3) to (6) the maximum angular velocity and magnetic field strength around BH could be estimated as

$$\Omega_\bullet = \frac{c^3}{GM_\bullet}\frac{a_\bullet}{2(1+\sqrt{1-a_\bullet^2})} \simeq 1.01 \times 10^5 m_\bullet^{-1} q \ {\rm rad\ s^{-1}} \quad (15)$$

and

$$B_{\bullet,{\rm p}} \simeq 2.4 \times 10^{14} L_{\rm X,iso,49}^{1/2} m_\bullet^{-1} q a_\bullet^{-2} X^{-1/2}(a_\bullet) \eta_{-2}^{-1/2} f_{\rm b,-2}^{1/2}\ {\rm G}. \quad (16)$$

With initial setup values, e.g., $m_\bullet = 3$ and a spin $a_\bullet = 0.9$, we have $B_{\bullet,{\rm p}} \sim 10^{14}$G and $\Omega_\bullet \sim 2.1 \times 10^4$ rad s^{-1}. In this case, the BH spin period is around 0.3 ms.

From Equations (9) to (10) the initial angular velocity and magnetic field at $r_{\rm ms}$ could be estimated as

$$\Omega_{\rm ms} \simeq 2.03 \times 10^5 m_\bullet^{-1}(\chi_{\rm ms}^3 + a_\bullet)^{-1} \ {\rm rad\ s^{-1}} \quad (17)$$

and

$$B_{\rm ms,p} \simeq 2.4 \times 10^{14} L_{\rm X,iso,49}^{1/2} (r_{\rm ms}/r_H)^{-5/4} m_\bullet^{-1} q a_\bullet^{-2} X^{-1/2}(a_\bullet) \eta_{-2}^{-1/2} f_{\rm b,-2}^{1/2}\ {\rm G} \quad (18)$$

With initial setup values, we have $B_{\rm ms,p} \sim 0.5 \times 10^{14}$G and $\Omega_{\rm ms} \sim 1.5 \times 10^4$ rad s^{-1}.

5. CONCLUSION AND DISCUSSION

As the first reported association between ultra-long GRBs and SNe, the GRB 111209A/SN 2011kl system provides us with a good chance to study the properties of central engines or even progenitors for ultra-long GRBs. In this work, we apply a fallback accretion scenario within the collapsar model to interpret the broadband data of GRB 111209A/SN 2011kl. We find that with all standard parameter values, both X-ray and optical observations could be well explained. In our interpretation, the central BH mass, the fallback material mass, and the SN ejecta mass are adopted as $3\,M_\odot$, $\sim 2.6\,M_\odot$, and $3\,M_\odot$, respectively, inferring that the total mass of the progenitor star is on the order of $10\,M_\odot$. Moreover, the outermost radius of the fallback material is estimated as $r_{\rm fb} \sim 3.2 \times 10^{11}$ cm, 5 times the solar radius. Therefore, we suggest that the progenitor of GRB 111209A is more likely a Wolf–Rayet star instead of a blue supergiant star, which is consistent with the observational implications from Greiner et al. (2015), although we argue that the central engine of this ultra-long burst is a BH rather than a magnetar. The required magnetic field strength around BH is $\sim 10^{14}$ G, similar to the magnetar magnetic field properties ($(6-9)) \times 10^{14}$G) as proposed by Greiner et al. (2015). But the BH spin period is around 0.3 ms, almost 2 orders of magnitude faster than the assumed magnetar spin (~12 ms).

If our interpretation is correct, the following implications can be inferred.

Under the framework of the collapsar model, the central engine (BH) activity timescale could have a wide range, depending not only on the size of the progenitor star but also on the stellar structure and rotation rate of the progenitor star (Kumar et al. 2008a, 2008b). The latter property would mainly affect the fallback process of the envelope material, which could largely extend the central engine activity time, having a chance to give rise to the ultra-long GRBs. On the other hand, the bounding shock responsible for the associated SN and the BP outflow from the initial accretion disk would transfer kinetic energy to the envelope materials. If the injected kinetic energy is less than the potential energy of the envelop material, the starting time of the fallback would be delayed, which may even prolong the burst duration. However, if the injected kinetic energy is larger, which might be the majority of cases,

[5] It is worth noting that the fitness of the GRB afterglow emission could also be achieved by simultaneously enhancing the kinetic energy but reducing the medium density, which means that E_k could be equal to or larger than 10^{53} erg (Nakauchi et al. 2013), matching with the isotropic gamma-ray energy release $E_{\gamma,{\rm iso}}$ in order of magnitude.

Table 1
Parameters for Interpreting the Broadband Data of GRB 111209A

BH and Ejecta Parameters						
	$M_\bullet$ ($M_\odot$)	$a_\bullet$	$M_{\rm ej}$ ($M_\odot$)	v/c	κ (cm^2 g^{-1})	
	3	0.9	3	0.06	0.06	
GRB Afterglow Parameters						
E_k (erg)	Γ_0	n (cm^{-3})	θ (rad)	ϵ_e	ϵ_B	p
7.6×10^{52}	200	1	0.4	0.1	10^{-4}	2.5
Other Parameters						
η	t_0 (s)	$t_{\rm p}$ (s)	$t_{\rm b}$ (s)	$\dot{M}_{\rm p}$ ($M_\odot$s^{-1})	α	κ_γ (cm^2 g^{-1})
0.05	$3000/(1+z)$	$8000/(1+z)$	$1.8 \times 10^4/(1+z)$	2.5×10^{-4}	5	0.1

the fallback process is vanished and the central engine activity is relatively short, corresponding to the normal long GRBs. It is worth noting that besides GRB 111209A, the other GRB that exhibits a fallback bump in an X-ray light curve, namely, GRB 121027A, is also an ultra-long burst (Wu et al. 2013).

Regardless of the fallback process, BP outflow would always deliver additional energy to the SN ejecta, which may explain the fact that GRB-associated SNe are usually energetic hypernovae (Li et al. 2016, for details). For ultra-long GRBs, where fallback accretion might occur, the associated SNe could be even brighter, like SN 2011kl, since the BP outflow injection is largely prolonged. It is worth noticing that given the ejecta properties, such as its radial density profile, metallicity content, and so on, the SN spectrum is essentially determined by the total injected energy from the central engine, no matter whether the central engine is a magnetar or a BH. For the case of SN 2011kl, Greiner et al. (2015) have carefully reproduced its spectrum within the magnetar central engine scenario and interpreted the observations. With the parameters presented in Table 1, it is easy to show that around the SN peak time (10^6 s), the total injected energy from the BP outflow is similar to the magnetar injection with parameters adopted in Greiner et al. (2015). We thus claim that the SN spectrum from our model is expected to be similar to the results calculated in Greiner et al. (2015).

During the fallback, the disk accretion rate ($\dot{M}_{\rm p} = 2.5 \times 10^{-4} M_\odot$ s^{-1}) is too low to ignite significant neutrino emission (Popham et al. 1999; Chen & Beloborodov 2007). As a concequence, the accretion flow could be dominated by advection at this stage, i.e., an ADAF, which has strong mass outflow due to its positive Bernoulli constant. Therefore, not all of the fallback mass accretes onto the BH. In contrast, the majority is ejected in the disk wind (Kumar et al. 2008a). MacFadyen & Woosley (1999) found that energy dissipation in the disk can launch a wind with significant ^{56}Ni. The study by Li et al. (2016) indicates that large ^{56}Ni mass is also produced in the magnetic outflow. This may give rise to the ^{56}Ni mass observed in the nebular spectra of hypernovae through Fe emission (e.g., Mazzali et al. 2001).

Numerical simulations suggested that the BZ mechanism can power highly collimated GRB jets. However, additional simulations will be needed to see whether the magnetically driven disk wind could drive a more isotropic hypernova blast.

We thank the referee for the helpful comments that have helped us to improve the presentation of the paper. This work is supported by the National Basic Research Program (973 Program) of China (grants 2014CB845800) and the National Natural Science Foundation of China under grants 11543005, U1431124, and 11361140349 (China–Israel joint program).

REFERENCES

Armitage, P. J., & Natarajan, P. 1999, ApJL, 523, 7
Arnett, W. D. 1982, ApJ, 253, 785
Bardeen, J. M., Press, W. H., & Teukolsky, S. A. 1972, ApJ, 178, 347
Blandford, R. D., & Payne, D. G. 1982, MNRAS, 199, 883
Blandford, R. D., & Znajek, R. L. 1977, MNRAS, 179, 433
Burrows, D. N., Romano, P., Falcone, A., et al. 2005, Sci, 309, 1833
Chatzopoulos, E., Wheeler, J. C., & Vinko, J. 2009, ApJ, 704, 1251
Chatzopoulos, E., Wheeler, J. C., & Vinko, J. 2012, ApJ, 746, 121
Chen, W.-X., & Beloborodov, A. M. 2007, ApJ, 657, 383
Chevalier, R. A. 1989, ApJ, 346, 847
Dai, Z. G., & Liu, R.-Y. 2012, ApJ, 759, 58
Fan, Y. Z., Zhang, B., & Proga, D. 2005, ApJL, 635, L129
Gal-Yam, A. 2012, Sci, 337, 927
Gao, H., Lei, W.-H., Zou, Y.-C., Wu, X.-F., & Zhang, B. 2013, NewAR, 57, 141
Gao, H., & Mészáros, P. 2015, ApJ, 802, 90
Gendre, B., Stratta, G. & On Behalf of the FIGARO Collaboration 2013, arXiv:1305.3194
Golenetskii, S., Aptekar, R., Mazets, E., et al. 2011, GCN, 12663, 1
Greiner, J., Mazzali, P. A., Kann, D. A., et al. 2015, Natur, 523, 189
Hoversten, E. A., Evans, P. A., Guidorzi, C., et al. 2011, GCN, 12632, 1
Kann, D. A., Klose, S., Kruehler, T., & Greiner, J. 2011, GCN, 12647, 1
King, A., O'Brien, P. T., Goad, M. R., et al. 2005, ApJL, 630, L113
Klotz, A., Gendre, B., Boer, M., & Atteia, J. L. 2011, GCN, 12633, 1
Kumar, P., Narayan, R., & Johnson, J. L. 2008a, MNRAS, 388, 1729
Kumar, P., Narayan, R., & Johnson, J. L. 2008b, Sci, 321, 376
Kumar, P., & Zhang, B. 2015, PhR, 561, 1
Lee, H. K., Wijers, R. A. M. J., & Brown, G. E. 2000, PhR, 325, 83
Lei, W. H., Wang, D. X., Zhang, L., et al. 2009, ApJ, 700, 1970
Lei, W. H., Wang, D. X., Zou, Y. C., & Zhang, L. 2008, ChJAA, 8, 404
Lei, W.-H., & Zhang, B. 2011, ApJL, 740, L27
Lei, W.-H., Zhang, B., & Liang, E.-W. 2013, ApJ, 765, 125
Levan, A. J., Tanvir, N. R., Starling, R. L. C., et al. 2014, ApJ, 781, 13
Li, L.-X. 2000, PhRvD, 61, 084016
Li, Y., Xie, W., Wang, D.-X., Gao, H., & Lei, W.-H. 2016, ApJ, submitted
Liang, E.-W., Zhang, B.-B., & Zhang, B. 2007, ApJ, 670, 565
Liu, T., Hou, S.-J., Xue, L., & Gu, W.-M. 2015, ApJS, 218, 12
Lyman, J. D., Bersier, D., James, P. A., et al. 2016, MNRAS, 457, 328
MacFadyen, A. I., & Woosley, S. E. 1999, ApJ, 524, 262
MacFadyen, A. I., Woosley, S. E., & Heger, A. 2001, ApJ, 550, 410
Margutti, R., Bernardini, G., Barniol Duran, R., et al. 2011, MNRAS, 410, 1064
Mazzali, P. A., Nomoto, K., Patat, F., & Maeda, K. 2001, ApJ, 559, 1047
McKinney, J. C. 2005, ApJL, 630, L5
Mészáros, P., & Rees, M. J. 2001, ApJL, 556, L37
Moderski, R., Sikora, M., & Lasota, J. P. 1997, in Proc. Int. Conf. on Relativistic Jets in AGNs, ed. M. Ostrowski et al. (Krakow: Jagiellonski University Astronomical Observatory), 110
Nakauchi, D., Kashiyama, K., Suwa, Y., & Nakamura, T. 2013, ApJ, 778, 67
Popham, R., Woosley, S. E., & Fryer, C. 1999, ApJ, 518, 356

Quimby, R. M., Kulkarni, S. R., Kasliwal, M. M., et al. 2011, Natur, 474, 487
Stratta, G., Gendre, B., Atteia, J. L., et al. 2013, ApJ, 779, 66
Troja, E., Cusumano, G., O'Brien, P. T., et al. 2007, ApJ, 665, 599
Virgili, F. J., Mundell, C. G., Pal'shin, V., et al. 2013, ApJ, 778, 54
Vreeswijk, P., Fynbo, J., & Melandri, A. 2011, GCN, 12648, 1
Wang, D. X., Xiao, K., & Lei, W. H. 2002, MNRAS, 335, 655
Wang, S. Q., Wang, L. J., Dai, Z. G., & Wu, X. F. 2015a, ApJ, 799, 107
Wang, S. Q., Wang, L. J., Dai, Z. G., & Wu, X. F. 2015b, ApJ, 807, 147
Wu, X.-F., Hou, S.-J., & Lei, W.-H. 2013, ApJL, 767, L36
Zhang, B., Fan, Y. Z., Dyks, J., et al. 2006, ApJ, 642, 354
Zhang, B., & Yan, H. 2011, ApJ, 726, 90
Zhang, B.-B., Zhang, B., Murase, K., Connaughton, V., & Briggs, M. S. 2014, ApJ, 787, 66
Zhang, W., Woosley, S. E., & Heger, A. 2008, ApJ, 679, 639